
The effect of conduction band nonparabolicity on binding energy of a GaAs quantum dot embedded at the center of a $\text{Ga}_{1-x}\text{Al}_x\text{As}$ nano-wire

Gh. Safarpour^{1,*}, M. Moradi², M. A. Izadi¹, M. Novzari¹ and E. Niknam¹

¹Zarghan Branch, Islamic Azad University, Zarghan, Iran

²Department of Physics, College of Sciences, Shiraz University, Shiraz 71454, Iran

E-mails: safarpour.ghasem@gmail.com

Abstract

The effects of conduction band nonparabolicity, aluminum concentration and external electric field on the charge density and binding energy of an on-center hydrogenic donor impurity in a spherical quantum dot which is located at the center of a cylindrical nano-wire are studied. The energy eigenvalues and the corresponding wave functions are calculated using finite difference approximation within the effective mass framework. The results reveal that the binding energies (I) decrease as the electric field increases, (II) become negligible for large values of electric field, (III) increase as the aluminum concentration increases and (IV) the conduction band nonparabolicity has a noticeable effect on the binding energy, and hence should be taken into account.

Keywords: Binding energy; Conduction band nonparabolicity; Electric field; Spherical quantum dot; Nano-wire

1. Introduction

Since the first investigation on the binding energy of a hydrogenic donor impurity within an infinite potential well (Bastard, 1981), there has been increasing interest on the electronic and optical properties of hydrogenic impurity confined by low-dimensional semiconductors. Existence of hydrogenic impurity influences not only on the electronic mobility, but also alters optical properties of nanostructures (Dalgic, 2005; Rezaei, 2011; Mathan Kumar, 2012; Liang, 2012). It has been found that the dimension reduction of the system results in strengthening the coulomb interaction, so the binding energy is larger in low dimensional systems (Dalgic, 2005; Nasri, 2010, Liang, 2011). An outstanding type of low dimensional semiconductors is quantum dot (QD), which has received a great deal of attention. In usage, QDs provide the opportunity of confining charge carriers in all spatial directions in electronic devices (Vaseghi, 2012; Xie, 2011). In nanofabrication progress, researchers were able to produce new generation of low dimensional semiconductors which are the combination of embedded QDs in a nano-wire. Owing to these combinational nanostructures, it is possible to manipulate devices based on low-dimensional semiconductors in order to reach desired properties (Safarpour, 2012; Safarpour, 2012).

Additionally, external perturbations significantly affect electronic and optical properties of the nanostructures. Applying external electric field, among other perturbations, has attracted many researchers. It is found that altering the direction or magnitude of electric field makes it possible to precisely modify electronic and optical features of system (He, 2010; Ulas, 1998; Gerardin Jayam, 2003; Rezaei, 2012).

In the field of electronic properties of semiconductor nanostructures, most of investigations are based on parabolic one band approximation. On the other hand, it is well known that energy dispersion relation is only parabolic around band edge (Rezaei, 2012). So, in a more realistic model, in order to accurately calculate the energy levels, it is essential to take nonparabolicity of conduction band into account (Rezaei, 2011; Nithiananthi, 2006; Bose, 2006; Mora-Ramos, 2012).

In the present work simultaneous effects of external electric field and conduction band nonparabolicity on the binding energy of an impure spherical QD embedded at the center of a cylindrical nano-wire are reported. Calculations are based on the effective mass approximation via finite difference method. The rest of this article is organized as follows. Theoretical approach and applied method are demonstrated in section (2) and numerical results and a brief summary are presented in Sections (3) and (4), respectively.

*Corresponding author

Received: 18 March 2014 / Accepted: 5 July 2014

2. Theory

We consider a GaAs spherical QD with radius R_1 , located at the center of a $\text{Ga}_{1-x}\text{Al}_x\text{As}$ cylindrical nano-wire with radius R_2 and height l . The origin is taken at the bottom of nano-wire and the z-axis is defined along nano-wire axis. In the energy dependent effective mass which accounts for the band nonparabolicity and in the cylindrical coordinates the Hamiltonian of a single particle in the presence of an external electric field can be expressed as

$$H(\rho, \phi, z) = -\frac{\hbar^2}{2m^*(E, \rho, z)} \left(\frac{\partial^2}{\partial \rho^2} + \frac{1}{\rho} \frac{\partial}{\partial \rho} + \frac{1}{\rho^2} \frac{\partial^2}{\partial \phi^2} + \frac{\partial^2}{\partial z^2} \right) + V(\rho, z) + eFz, \quad (1)$$

The electric field is assumed to be in the z-direction and the particle confining potential, $V(\rho, z)$, is given by

$$V(\rho, z) = \begin{cases} 0 & \sqrt{\rho^2 + (z-l/2)^2} < R_1 \\ v & \sqrt{\rho^2 + (z-l/2)^2} > R_1 \text{ \& } \rho \leq R_2 \text{ \& } 0 \leq z \leq l \end{cases}, \quad (2)$$

here $v = Q_c(E_g^{\text{GaAl}_x\text{As}} - E_g^{\text{GaAs}})$, E_g is the band-gap energy and Q_c is the band offset ratio (Herbert, 2000). The nonparabolicity of the conduction band (Cooper, 2010) is considered through the energy dependent effective mass as

$$\frac{1}{m^*(E, \rho, z)} = \frac{1}{m^*(\rho, z)} \frac{1}{\{1 + \alpha(\rho, z)[E - V(\rho, z)]\}} \quad (3)$$

where E is the particle energy, $V(\rho, z)$ is the confining potential, $m^*(\rho, z)$ is the band edge effective mass and $\alpha(\rho, z)$ is the nonparabolicity parameter which quantifies the effect of nearby energy bands on the particle dispersion relation. Here we use the simplest form of the nonparabolicity i.e. $\alpha = 1/E_g$ (Cooper, 2010).

We are interested in finding ground and first excited states. Since our geometry has axial symmetry, the azimuthal part of the wave function can be separated as $F_m(\phi) = \frac{1}{\sqrt{2\pi}} e^{im\phi}$. It is worth pointing out that we just calculate the electron energy levels for $m=0$. Therefore, the Schrodinger equation can be rewritten as:

$$\left\{ -\frac{\hbar^2}{2m^*(E, \rho, z)} \left(\frac{\partial^2}{\partial \rho^2} + \frac{1}{\rho} \frac{\partial}{\partial \rho} + \frac{\partial^2}{\partial z^2} \right) + V(\rho, z) + eFz \right\} \Psi(\rho, z) = E\Psi(\rho, z), \quad (4)$$

The Schrodinger equation is numerically solved by the finite difference (FD) approximation (Cooper, 2010; Wayan Sudiarta, 2007; Amiraliev, 2005). In order to carry out simulation numerically, one needs to discretize Eq. (4) using FD schemes. First, it should be noted that to avoid achieving huge matrix, the non-uniform space discretization is considered for z-coordinate with aspect ratio

$$\frac{\Delta z_{j+1}}{\Delta z_j} = \frac{z_{j+1} - z_j}{z_j - z_{j-1}} = 1.1. \text{ For } \rho\text{-coordinate a}$$

uniform space discretization is applied. The spatial derivative is approximated by the central FD scheme for all discretized space except on boundaries and is given by

$$\begin{aligned} & \frac{1}{m^*(E, \rho, z)} \left(\frac{\partial^2}{\partial \rho^2} + \frac{1}{\rho} \frac{\partial}{\partial \rho} + \frac{\partial^2}{\partial z^2} \right) \\ & + V(\rho, z) + eFz \psi^{(in,out)}(\rho, z) \cong \\ & \frac{1}{m^*(E, \rho_i, z_j) \Delta \rho^2} (\psi^{(in,out)}(i+1, j) - \\ & 2\psi^{(in,out)}(i, j) + \psi^{(in,out)}(i-1, j)) + \\ & \frac{1}{m^*(E, \rho_i, z_j) \rho \Delta \rho} (\psi^{(in,out)}(i+1, j) - \\ & \psi^{(in,out)}(i, j)) + \frac{1}{m^*(E, \rho_i, z_j) \Delta z_j^2} \times \\ & (\psi^{(in,out)}(i, j+1) - 2\psi^{(in,out)}(i, j) + \\ & \psi^{(in,out)}(i, j-1)) + (V(i, j) + eFz_j) \psi^{(in,out)}(i, j), \end{aligned} \quad (5)$$

The notation $\psi^{(in,out)}(i, j) \equiv \psi^{(in,out)}(i\Delta\rho, z_j + \Delta z_j)$ (where $\Delta\rho$ and Δz_j are spatial spacing) is used in this paper and the superscriptions “in” and “out” represent the wave function inside and outside the dot. For discretized space on different boundaries, different FD schemes should be used (Ozturk, 2004) as follows: (I) for boundary ($\forall \rho, z=0$) the forward FD scheme is applied, (II) for boundary ($\forall \rho, z=l$) the backward FD scheme is applied, (III) for boundary ($\rho=0, \forall z$) the forward FD scheme is used for ρ -coordinate and the central FD scheme for z -coordinate, (IV) for boundary ($\rho=R_2, \forall z$) the backward FD scheme is used for ρ -coordinate.

The Dirichlet boundary condition (i.e., infinite potential barrier) has been imposed at the nano-wire boundaries. The continuity of the wave function

and its derivative on the QD boundary ($\sqrt{\rho^2 + (z-l/2)^2} = R_1$) are imposed and are considered by appropriate FD schemes. In order to linearize the coefficient matrix we use the same method which has been introduced by Cooper et al. (Cooper, 2010). Additionally, we use the same assumption to identify the physical eigenvalues, i.e.: (I) discarding complex eigenvalues which arise due to considering nonparabolicity and asymmetry in coefficient matrix, (II) discarding the real states whose energies exceed the maximum confining potential. These states are usually not of interest and can be discarded based on their energy (Cooper, 2010).

3. Numerical results and discussion

In this study, we have numerically calculated the electronic structures of a GaAs spherical quantum dot which is located at the center of a $\text{Ga}_{1-x}\text{Al}_x\text{As}$ cylindrical nano-wire under effects of external electric field and conduction band nonparabolicity. Electronic wave functions and energy eigenvalues are calculated by FD approximation. The numerical method used in this paper is the same as the one applied in Safarpour et al. (2014). In that paper the error tolerance was reported and the obtained results were compared with both analytical and computed results by finite element method. The parameters used in the present work are as follows (Herbert Li, 2000; Cooper, 2010): $m_{\text{Ga}_x\text{Al}_{1-x}\text{As}}^*/m_0 = 0.0632 + 0.0856x + 0.0231x^2$, $E_g^{\text{Ga}_x\text{Al}_{1-x}\text{As}} = 1.424 + 1.519x + x(1-x)(0.127 - 1.310x)$, $Q_c = 0.7$ and $\epsilon_r = 13.18$. In our calculation we have used the following units: meV for energy, nm for length and KV/cm for electric field.

In all numerical calculations, the validity of the method should be confirmed. One way to check the accuracy of the produced wave functions is to test the orthogonality between states which are exactly orthogonal. For solving an eigenvalue problem with FD approximation, the first step is to discretize space and apply different FD schemes (Mora-Ramos, 2012). This discrete approximation leads to finite-dimensional matrix representation. In the present method for the geometry with parameters $R_1 = 5nm$, $R_2 = 20nm$ and $l = 400nm$, the dimensions of the coefficient matrix are 6551×6551 . For parabolic band approximation the absolute values of orthogonality between ground and first excited states, $|\langle 1s | 2p \rangle|$, is equal to 7.24622×10^{-11} and 10.01990×10^{-11} for $F = 0KV/cm$ and $F = 10KV/cm$, respectively.

As mentioned in Cooper et al's work (Cooper, 2010) the nonparabolicity inherently introduces nonorthogonality. However, in present work the orthogonality between ground and first excited states is also calculated for nonparabolic band approximation and is equal to 4.64734×10^{-8} and 2.22695×10^{-8} for $F = 0KV/cm$ and $F = 10KV/cm$, respectively. It is clear that, even for nonparabolic band approximation, calculated wave functions by the presented method are as reliable as expected.

We should mention that in many articles, the nonparabolic band approximation has been considered for confined region by QD (Rezaei, 2012; Bose, 2006). In present work the binding energies of ground state (1s) and first excited state (2p) are calculated for the case that nonparabolicity is considered in both dot and nano-wire region and obtained results are compared with parabolic band approximation.

First, consider charge density. Figures 1 and 2 show the charge distribution along nano-wire axis in presence and absence of hydrogenic impurity, parabolic and nonparabolic band approximations and for two different values of electric field strengths $F = 0$ and $F = 10KV/cm$. As we can see from Fig. 1, in the absence of electric field the charge distribution is symmetric and concentrated around the origin of the QD ($z = 200nm$) in both cases of presence or absence of hydrogenic impurity. In absence of hydrogenic impurity the first confinement (quantum confinement of dot) is dominant factor, leading to carrier localization inside the dot. The effect of impurity increases probability of finding electron around the origin. Moreover, the effect of nonparabolicity parameter (see Eq. 3) increases energy eigenvalues and consequently causes an increment in the charge distribution. As mentioned above the direction of electric field is assumed to be along the nano-wire axis (+z). Then, applying electric field causes an asymmetry in charge density and forces the electron to localize at the bottom of nano-wire. Additionally, it is also shown that presence of impurity is diminished by applying an electric field, because of the dominant effect of electric field in comparison to Coulomb interaction.

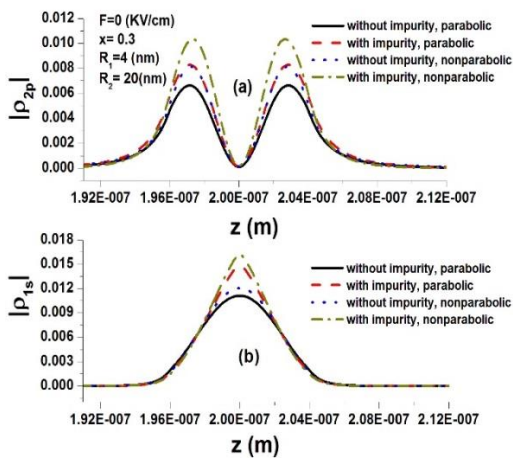


Fig. 1. The charge distribution along the nano-wire axis in presence and absence of hydrogenic donor impurity for parabolic and nonparabolic band approximations in absence of external electric field

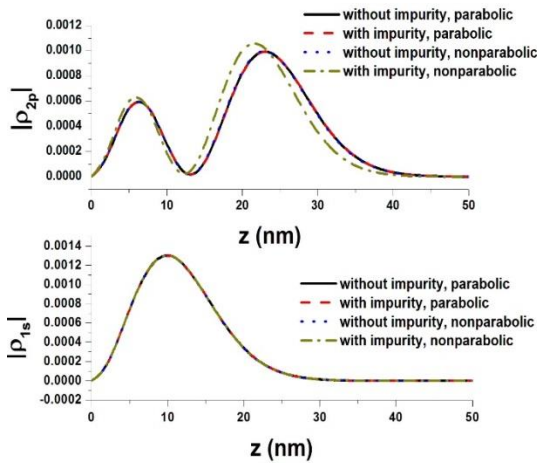


Fig. 2. The charge distribution along the nano-wire axis in presence and absence of hydrogenic donor impurity for parabolic and nonparabolic band approximations for two different values of external electric field

Figures 3(a) and 3(b) display variations of binding energies of 1s and 2p states as a function of dot radius for both parabolic and nonparabolic band approximations in the absence and presence of external electric field. The figures show that, the binding energies of ground and first excited states are increased by increasing dot radius. The origin of this behavior is that by increasing the dot radius electronic wave functions become more localized inside the dot region which enhances the binding energy. By further increasing the dot radius an opposite behavior is observed and binding energies are decreased. For large values of dot radius, electron is mostly localized inside the dot. Hence, with an augment in dot radius the expectation value of electron-impurity distance increases, therefore, binding energy decreases. Additionally, the influence of band edge nonparabolicity is negligible

for small and large dot radii for ground state binding energy, which causes a decrement in binding energy for intermediate dot radii. For first excited state the peak value of binding energy is shifted toward lower dot radii by taking into account the effect of nonparabolic band approximation. Furthermore, the effect of nonparabolicity is more obvious for first excited state.

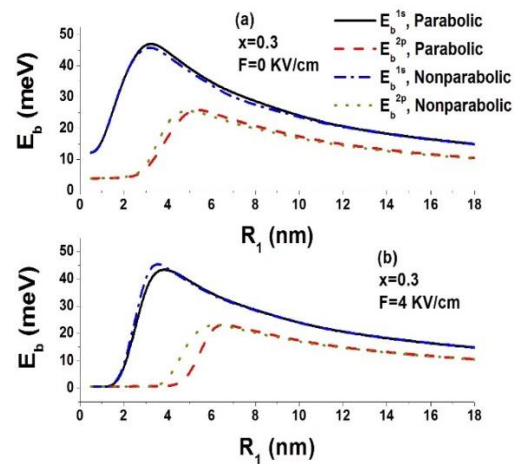


Fig. 3. The variation of the binding energy of ground and first excited states as a function of the dot radius for both parabolic and nonparabolic band approximations (a) in the absence and (b) presence of electric field

In order to investigate the effect of wire radius on electronic structure of the system, in Fig. 4 the ground and first excited states binding energies are plotted as a function of nano-wire radius in absence ($F = 0 \text{ KV/cm}$) and presence ($F = 4 \text{ KV/cm}$) of external electric field for both parabolic and nonparabolic band approximations. The following points can be concluded from this Fig. (I). For small nano-wire radius, the effect of nano-wire confinement forces electron to remain in the dot region. As nano-wire radius, increases, the effect of second confinement becomes weaker and thus binding energies decrease. (II) In presence of electric field and for the ground state the first confinement (QD confinement) and second confinement (nano-wire) are dominant factors. Therefore, for large values of nano-wire radius binding energy of ground state approaches 44 meV even in presence of external electric field. (III) In presence of electric field and for first excited state the second confinement is a determining factor. For small values of nano-wire radius, the electron is mostly localized around the impurity. Therefore, first excited state binding energy is not negligible. By increasing the nano-wire radius the effect of second confinement becomes negligible and hence presence of external electric field causes an increment in probability distribution of finding electron at the bottom of nano-wire. So, expectation value of electron-impurity distance increases which causes a

decrement in first excited state binding energy. Additionally, in presence of electric field, the binding energy of first excited state becomes negligible for large value of nano-wire radius.

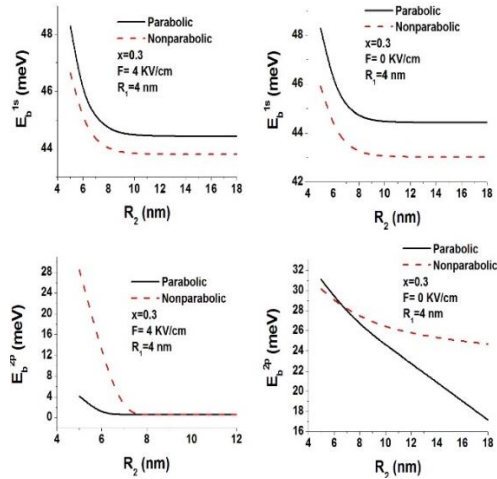


Fig. 4. Ground and first excited state binding energies as a function of nano-wire radius in presence and absence of external electric field for a given value of dot radius

Figure 5 shows the variation of binding energies of 1s and 2p states as a function of electric field strength in both parabolic and nonparabolic band approximations. This figure indicates that binding energies rapidly decrease with an augment in electric field strength and remain constant by further increasing of the electric field. In order to explain this behavior we note that at zero electric field electron is mostly localized inside the dot. By increasing electric field, the charge distribution of electron shifts away from the impurity. Therefore, the expectation value of electron-impurity distance increases which leads to a decrement in binding energy. For large values of electric field, electron is localized at the bottom of nano-wire; hence, further increasing of the electric field has no effect on the binding energies.

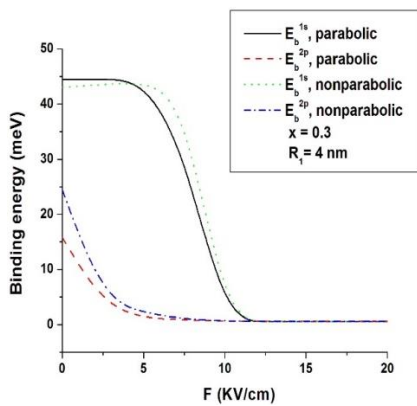


Fig. 5. The variation of the binding energies of ground and first excited states as a function of the electric field strength in both parabolic and nonparabolic band approximations

The effect of the Al concentration on the binding energies of a donor impurity is presented in Fig. 6 for both parabolic and nonparabolic band approximations. It is clear that an increase in Al concentration results in an increment in the binding energy. It is a direct consequence of the effect of Al concentration on the confining potential. By increasing Al concentration the electron wave functions are more strongly localized inside the QD, thus, the Coulomb interaction is enhanced and then donor binding energy increases. Additionally, the effect of band edge nonparabolicity is to decrease (increase) the binding energy for ground state (first excited state). Again, the effect of nonparabolicity approximation is more striking for the first excited state.

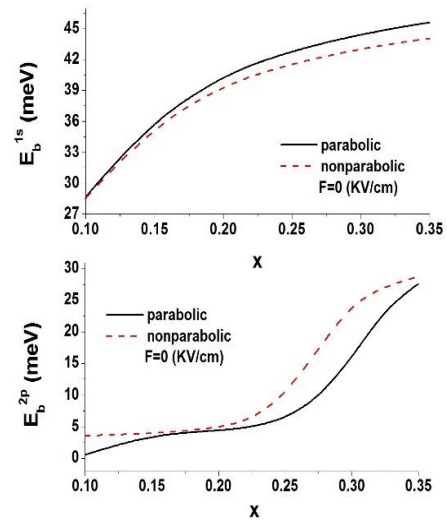


Fig. 6. The variation of the binding energies of ground and first excited states as a function of the Al concentration in both parabolic and nonparabolic band approximations

4. Conclusion

In conclusion, we have calculated the ground and first excited states charge density and binding energies of an on-center hydrogenic donor impurity in a spherical QD located at the center of a cylindrical nano-wire under the influence of applied electric field and Al concentration for parabolic and non-parabolic band approximations. The binding energies of ground and first excited state are studied as a function of dot radius, electric field, and Al concentration. The result shows that (I) as the dot radius increases the binding energies of ground and first excited states show a maximum value. (II) For small or large values of electric field strength, as the electric field increases the binding energies of ground state remains constant but for intermediate electric field strength, it decreases by increasing

electric field. For the first excited state, binding energy decreases and becomes negligible as the electric field strength increases. (III) The binding energies of ground and first excited states increase as the Al concentration increases.

References

- Amiraliyev, G. M. (2005). The convergence of a finite difference method on layer-adapted mesh for a singularly perturbed system. *A. Math. Comput.*, 162, 1023–1034.
- Bastard, G. (1981). Hydrogenic impurity states in a quantum well: A simple model. *Phys. Rev. B*, 24, 4714.
- Bose, C., Midya, K., & Bose, M. K. (2006). Effect of conduction band non-parabolicity on the donor states in GaAs-(Al,Ga)As spherical quantum dots. *Physica E*, 33, 116–119.
- Cooper, J. D., Valavanis, A., Ikonic, Z., Harrison, P., & Cunningham, J. E. (2010). Finite difference method for solving the Schrödinger equation with band nonparabolicity in mid-infrared quantum cascade lasers. *J. Appl. Phys.* 108, 113109.
- Dalgic, S., Ulas, M., & Ozkapi, B. (2005). Electric field effect on the binding energy of a nonhydrogenic donor impurity in a square quantum well wire. *J. Optoelectron. Adv. M.*, 7, 2041–2046.
- Gerardin Jayam, Sr., & Navaneethakrishnan, K. (2003). Effects of electric field and hydrostatic pressure on donor binding energies in a spherical quantum dot. *Solid State Commun.*, 126, 681–685.
- He, L., & Xie, W. (2010). Effects of an electric field on the confined hydrogen impurity states in a spherical parabolic quantum dot. *Superlattice Microst.*, 47, 266–273.
- Herbert Li, E. (2000). Material parameters of InGaAsP and InAlGaAs systems for use in quantum well structures at low and room temperatures. *Physica E*, 5, 215–273.
- Liang, S. J., Xie, W. F., Sarkisyan, H. A., Meliksetyan, A. V., & Shen, H. (2012). Electronic and optical properties of a nanoring in the presence of external magnetic field. *Superlattice Microst.*, 51, 868–876.
- Liang, S. J., & Xie, W. F. (2011). The hydrostatic pressure and temperature effects on a hydrogenic impurity in a spherical quantum dot. *Eur. Phys. J. B*, 81, 79–84.
- Mathan Kumar, K., John Peter, A., & Lee, C. W. (2012). Optical properties of a hydrogenic impurity in a confined Zn_{1-x}Cd_xSe/ZnSe spherical quantum dot. *Superlattice Microst.*, 51, 184–193.
- Mora-Ramos, M. E., Duque, C. A., Kasapoglu, E., Sari, H., & Sokmen, I. (2012). Linear and nonlinear optical properties in a semiconductor quantum well under intense laser radiation: Effects of applied electromagnetic fields. *J. Lumin.*, 132, 901–913.
- Nasri, D., & Sekkal, N. (2010). General properties of confined hydrogenic impurities in spherical quantum dots. *Physica E*, 42, 2257–2263.
- Nithiananthi, P., & Jayakumar, K. (2006). Effect of Γ -X band crossover and impurity location on the diamagnetic susceptibility of a donor in a quantum well. *Solid State Commun.*, 138, 305–308.
- Ozturk, E., Sari, H., & Sokmen, I. (2004). The dependence of the intersubband transitions in square and graded QWs on intense laser fields. *Solid State Commun.*, 132, 497–502.
- Rezaei, G., Vahdani, M. R. K., & Vaseghi, B. (2011). Nonlinear optical properties of a hydrogenic impurity in an ellipsoidal finite potential quantum dot. *Curr. Appl. Phys.*, 11, 176–186.
- Rezaei, G., & Doostimotlagh, N. A. (2012). External electric field, hydrostatic pressure and conduction band non-parabolicity effects on the binding energy and the diamagnetic susceptibility of a hydrogenic impurity quantum dot. *Physica E*, 44, 833–838.
- Rezaei, G., Doostimotlagh, N. A., & Vaseghi, B. (2011). Conduction band non-parabolicity effect on the binding energy and the diamagnetic susceptibility of an on-center hydrogenic impurity in spherical quantum dots. *Physica E*, 43, 1087–1090.
- Safarpour, Gh., Moradi, M., & Barati, M. (2012). Hydrostatic pressure and temperature effects on the electronic energy levels of a spherical quantum dot placed at the center of a nano-wire. *Superlattice Microst.*, 52, 687–696.
- Safarpour, Gh., Barati, M., & Moradi, M. (2012). Electron-hole transition in a spherical quantum dot confined at the center of a cylindrical nano-wire: Comparison of isotropic and anisotropic effective mass. *Superlattice Microst.*, 52, 669–677.
- Safarpour, Gh., Novzari, M., Izadi, M. A., Niknam, E., & Barati, M. (2014). Binding energy and nonlinear optical properties of an on-center hydrogenic impurity in a spherical quantum dot placed at the center of a cylindrical nano-wire: Comparison of hydrogenic donor and acceptor impurities. *Physica B*, 436, 117–125.
- Ulas, M., & Akbas, H. (1998). Shallow Donors in a Quantum Well Wire; Electric Field and Geometrical Effects. *Tr. J. Physics*, 22, 369–375.
- Vaseghi, B., & Sajadi, T. (2012). Simultaneous effects of pressure and temperature on the binding energy and diamagnetic susceptibility of a laser dressed donor in a spherical quantum dot. *Physica B*, 407, 2790–2793.
- Wayan Sudiarta, I., & Wallace Geldart, D. J. (2007). Solving the Schrodinger equation using the finite difference time domain method. *J. Phys. A: Math. Theor.*, 40, 1885–1896.
- Xie, W. F., & Liang, S. J. (2011). Optical properties of a donor impurity in a two-dimensional quantum pseudodot. *Physica B*, 406, 4657–4660.